Intraseasonal Variability of Summer Precipitation in Mexico: MJO Influence on the Midsummer Drought

JULIET PERDIGÓN-MORALES

Posgrado en Ciencias de la Tierra, Centro de Ciencias de la Atmósfera, Universidad Nacional Autónoma de México, Mexico City, Mexico

ROSARIO ROMERO-CENTENO

Centro de Ciencias de la Atmósfera, Universidad Nacional Autónoma de México, Mexico City, Mexico

BRADFORD S. BARRETT

Oceanography Department, U.S. Naval Academy, Annapolis, Maryland

PAULINA ORDOÑEZ

Centro de Ciencias de la Atmósfera, Universidad Nacional Autónoma de México, Mexico City, Mexico

(Manuscript received 29 June 2018, in final form 28 January 2019)

ABSTRACT

The aim of this study is to understand how the Madden–Julian oscillation (MJO) modulates the bimodal seasonal rainfall distribution across the regions in Mexico where the midsummer drought (MSD) occurs. The MSD is characterized by a precipitation decrease in the middle of the rainy season. Relative frequencies of each active phase of the Real-time Multivariate MJO index were calculated at each grid point in the high-resolution Climate Hazards Group Infrared Precipitation with Stations (CHIRPS) rainfall dataset for the first (MAX1) and second (MAX2) rainfall peaks and the MSD minimum (MIN). In addition, standardized anomalies of precipitation (from the CHIRPS dataset) and 300-hPa omega, 500-hPa geopotential height, and 850-hPa u- and v-wind components (from the Climate Forecast System Reanalysis) were calculated for each MJO phase and each month in the rainy season. Results show that the MIN (MAX2) occurs more frequently during the dry (wet) MJO phases, while the MJO seems not to influence MAX1 significantly. Anomalous anticyclonic (cyclonic) circulations at 850 hPa, positive (negative) 500-hPa geopotential height anomalies, northeast (southwest) 850-hPa wind anomalies over southern Mexico, and a low-level westward (eastward) flow in the northeastern tropical Pacific support the MIN (MAX2) pattern under the influence of the dry (wet) MJO phases. These features are more clearly observed in the MSDs of 1- and 2-month duration and over the southern half of Mexico. The results suggest that the bimodal distribution is less influenced by the MJO in regions of northeastern Mexico.

1. Introduction

The annual rainfall cycle over central and southern Mexico and Central America (e.g., Magaña et al. 1999; Amador et al. 2006; Gamble et al. 2008) and some regions of northern Mexico (Curtis 2002; Small et al. 2007; Karnauskas et al. 2013; Perdigón-Morales et al. 2018) has been well documented. In general, rainfall in these areas exhibits a bimodal behavior, in which the first and second maxima of precipitation occur during May–June and September–October, respectively, and a relative minimum of precipitation occurs in between. This relative reduction in rainfall during July–August is known as the midsummer drought (MSD; Magaña et al. 1999).

The duration and intensity of the MSD show high spatial and temporal variability in Mexico, Central America, and the Caribbean basin (e.g., Curtis and Gamble 2008; Maldonado et al. 2016; Perdigón-Morales et al. 2018). The physical forcing mechanisms associated with the bimodal precipitation pattern and its variability are complex, primarily because of the simultaneous

influence of different processes, both local and large scale. Moreover, the processes implicated in the occurrence of MSD on the Pacific side are different from those on the Caribbean (Herrera et al. 2015; Maldonado et al. 2016). The MSD's spatial and temporal characteristics have been explained in terms of seasonal changes in incoming solar radiation, sea surface temperature (SST), and low-level winds (Magaña et al. 1999); the variability of the position and strength of the intertropical convergence zone (ITCZ) and of the North Atlantic subtropical high pressure system (NASH) (e.g., Giannini et al. 2000; Mapes et al. 2005; Romero-Centeno et al. 2007; Small et al. 2007; Gamble et al. 2008); the intensification of the Caribbean low-level jet (CLLJ) and associated direct circulations and SST variability (e.g., Magaña and Caetano 2005; Herrera et al. 2015); and insolation variability caused by the biannual crossing of the solar declination (Karnauskas et al. 2013). All of these processes interact with, and are likely modulated by, larger-scale modes of atmospheric and oceanic variability. The focus of this study is to explore the influences of the tropical Madden–Julian oscillation (MJO) on this bimodal rainfall pattern.

The MJO is the most important mode of tropical intraseasonal variability, and it is characterized by a large-scale coupled pattern of atmospheric circulation and deep convection propagating eastward from the Indian Ocean along the equator with a period of 30–60 days (Madden and Julian 1994; Hendon and Salby 1994). The MJO has significant effects on the atmospheric circulation throughout the global tropics, although it also causes variations in the weather and climate of extratropical locations around the globe (e.g., Bond and Vecchi 2003; Zhang 2005). The MJO has been shown to modulate intraseasonal rainfall in the Western Hemisphere, including in the United States (Zhou et al. 2012), Central America (Barlow and Salstein 2006), the Caribbean (Martin and Schumacher 2011; Curtis and Gamble 2016), South America (Barrett et al. 2012; Alvarez et al. 2016; Shimizu et al. 2017), and Mexico (Barlow and Salstein 2006; Barrett and Esquivel 2013). Those studies found that the MJO's impact on precipitation can be traced to its modulation of the large-scale tropospheric circulation, generally oscillating between favorable and unfavorable conditions for upward vertical motion and convection. Indeed, Mo (2000) observed a clear impact of the MJO on precipitation over Mexico and found an oscillatory mode with a period of about 36–40 days in the 200-hPa divergence and outgoing longwave radiation anomalies. Low-level winds over Mexico and Central America have also been shown to vary with the MJO (e.g., Higgins and Shi 2001). With the exception of Curtis and Gamble (2016), who showed a relationship between the MJO and the Caribbean MSD (including southern Mexico), none of the abovementioned studies explored the potential modulation

of the MSD in Mexico by the MJO, although it is known that both the MJO and MSD exert a strong intraseasonal influence on precipitation in the region.

Maloney and Esbensen (2003) suggest a coupled feedback between convection and the low-level circulation over the east Pacific warm pool during the June–November MJO life cycle, where MJO convection may strengthen the local circulation during active convective periods, thereby increasing surface latent heat flux and convergence anomalies. It is plausible, then, that this is a physical mechanism by which the MJO influences precipitation during the MSD. Indeed, Romero-Centeno et al. (2007) found a high correlation between variations in precipitation rates from June through September in southern Mexico and Central America and variations in the low-level zonal wind in the northeastern tropical Pacific (NETP), with the maximum of precipitation in June and September coinciding with strong surface westerlies over the central NETP. More recently, variations in anomalous lower-troposphere westerlies and easterlies on the daily time scale in this region of the Pacific Ocean during summer have shown to be key elements of the MJO dynamics in the Pacific warm pool (Whitaker and Maloney 2018).

In addition, the summer rainfall regime in Mexico is highly influenced by the tropical cyclone activity in both the North Atlantic and the northeast Pacific basins. Some studies suggest that the MJO modulates the intraseasonal variability of convective activity over the tropical oceans, and can significantly modulate hurricane activity over the eastern Pacific (e.g., Maloney and Hartmann 2000a; Crosbie and Serra 2014) and North Atlantic Oceans (e.g., Maloney and Hartmann 2000b; Barrett and Leslie 2009; Klotzbach 2010).

Within this context, the question then becomes: Does the MJO contribute to the first and second rainfall maxima and to the MSD minimum? The primary goal of this study, therefore, is to examine the association between the leading global mode of intraseasonal variability and the summer rainfall in Mexico. Specifically, the analysis focuses on the role of the MJO in modulating the rainfall maxima at the beginning and end of the season and the minimum during the MSD in Mexico. It is worth noting that MJO–MSD cause–effect relationships are not directly explored here. In the next section, a description of the data, the MJO index, and the analysis methodology is given. The results of the study are presented in section 3, and section 4 contains the discussion and conclusions of these results.

2. Data and analysis procedures

The Real-time Multivariate MJO index (RMM; Wheeler and Hendon 2004) was used in this study as a measure of the MJO activity. This index has been widely

used in the literature (e.g., Martin and Schumacher 2011; Zhou et al. 2012; Barrett and Esquivel 2013; Ordoñez et al. 2013; Crosbie and Serra 2014) because it offers several advantages, including that it is a seasonally independent index, it effectively captures the propagation of the MJO convection around the globe, and the annual cycle and low-frequency variability associated with ENSO are removed before its calculation. The RMM index contains daily values of amplitude and phase as measures of the magnitude and location of the convective activity within the MJO life cycle, respectively. There are eight phases of the index, each providing an approximate location of the MJO active phase as it propagates eastward from the Indian Ocean. Phases 2 and 3 are associated with enhanced convection over the Indian Ocean, phases 4 and 5 over the Maritime Continent, phases 6 and 7 over the western Pacific, and phases 8 and 1 over the Western Hemisphere. Because a portion of Mexico is situated in a subtropical latitude zone, and because the tropical convection of the MJO in boreal summer nearly approaches the southern coast of Mexico, direct associations (i.e., no temporal lags) between the MJO phase and precipitation were explored here, similar to Barrett and Raga (2016).

Both active and inactive MJO days were considered in this study. An active (inactive) MJO day was defined as one in which the amplitude of the index is greater (less) than 1. Two MJO intensity categories were also examined following the classification proposed by Lafleur et al. (2015) in order to analyze if intensity variations have some influence as well. In this way, the MJO days were divided into active, when $1 \leq RMM < 1.5$, and very active, when $1.5 \leq RMM < 2.5$. The extremely active category ($RMM \geq 2.5$) was not included because the analysis has been broken down to monthly time scales and, consequently, the number of cases for each month in this category is very low, even null in some cases. In general, the patterns obtained for these intensity categories are similar to those of all active days ($RMM \geq 1$).

Previous studies have analyzed the MJO influence on summer precipitation in Mexico considering the July–September (or June–September) period jointly (Barlow and Salstein 2006; Barrett and Esquivel 2013). However, as previously stated, the summer precipitation in Mexico shows high intraseasonal variability, with important differences in monthly rainfall during each of the rainy months (from May to October). To gain insight into these monthly differences, the spatiotemporal variability of precipitation by MJO phase was analyzed separately for each of the summer months. For this purpose, daily precipitation data from the Climate Hazards Group Infrared Precipitation with Stations (CHIRPS; Funk et al. 2015) database were used. CHIRPS contains precipitation data in a quasi-global grid covering 50°S–50°N, 180°E–180°W
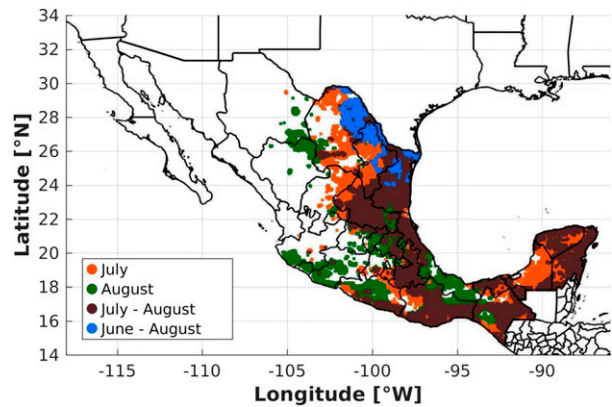

FIG. 1. Spatial pattern of the duration of the MSD in Mexico according to the high-resolution CHIRPS dataset for the period 1981–2010 (from Perdigón-Morales et al. 2018).

at a very high spatial resolution (0.05° × 0.05°) and several temporal resolutions (daily, pentad, and monthly). This relatively new database has shown to perform well in several regions of the world (e.g., López-Carr et al. 2015; Katsanos et al. 2016; Paredes-Trejo et al. 2016; Verdin et al. 2016). Recently, Perdigón-Morales et al. (2018) showed that CHIRPS acceptably reproduces the rainfall patterns in Mexico, especially the characteristics of the MSD.

Anomaly composites were used to analyze the temporal and spatial variability of the precipitation throughout the rainy season in Mexico, according to different MJO phases. A composite was generated for each phase of the MJO, and for each month of the rainy season (from May to October). Standardized anomalies were calculated at each grid point and the Monte Carlo technique was applied to test the statistical significance of all MJO composites, following Efron and Tibshirani (1994) with 10 000 iterations. Only the gridpoint anomalies that were statistically significant at the 95% confidence level are displayed.

The spatial MSD features obtained from Perdigón-Morales et al. (2018) are used to investigate the influence of the MJO on the seasonal precipitation pattern in the region where MSD occurs in Mexico. They defined four MSD types, depending on the following: 1) the dates of the first and second precipitation peaks (hereafter MAX1 and MAX2, respectively), and 2) the duration of the MSD. The first two types of MSD include cases in which the precipitation deficit occurs in 1 month (either July or August); the third type includes the case in which the MSD covers 2 months (July and August); and the fourth type includes the case in which it covers 3 months (from June to August). The spatial distribution of the MSD types over Mexico is shown in Fig. 1, which is defined as the MSD region. Similar to that study, here

MAX1 is defined as follows: 1) MAX1 occurs in May for the June–August MSD, 2) MAX1 occurs in June for both the July-only MSD and the July–August MSD, and 3) MAX1 occurs in July for the August-only MSD. As for MAX2, it is defined as follows: MAX2 occurs in August for the July-only MSD, and in September or October for the other three types of MSD. According to Perdigón-Morales et al. (2018), precipitation in September is always higher than August for the August-only MSD, always higher than July and August for the 2-month MSD, and always higher than June, July, and August for the 3-month MSD. However, October could also be identified as a MAX2 month, because October precipitation could be higher than September.

At each grid point, the dates of the MAX1, MIN, and MAX2 were identified during the rainy months for each year following Perdigón-Morales et al. (2018). The pentad (5-day) product of CHIRPS was used for this step. The precipitation time series were smoothed linearly at each grid point using a six-pentad running average. In this way, the filtered series were relatively insensitive to individual synoptic or mesoscale disturbances. Then, the years in which MSD occurred during the study period were identified. Note that, as seen in Perdigón-Morales et al. (2018), a reduction in precipitation associated with the MSD does not necessarily occur at every grid point each year. However, when MSD occurred, the dates of the MAX1 and MAX2 were identified selecting the pentad of maximum accumulation during the months of maximum precipitation (rainfall peak months), while the date of the MIN was identified selecting the pentad of minimum accumulation during the month(s) of minimum precipitation [the MSD month(s)]. Then, the dates of MAX1, MIN, and MAX2 were binned according to the active MJO phase present at the middle day of the pentad, and the relative frequencies of each MJO phase were calculated for each date. Finally, the statistical significance of the frequencies obtained for each MJO phase was tested at the 95% level, following the methodology of Hall et al. (2001). The most frequent and statistically significant MJO phase for each grid point was identified, and its frequency distribution in the MSD region in Mexico was analyzed.

The atmospheric circulation patterns prevalent during the different MJO phases during the rainy season months were analyzed. For this purpose, 6-hourly gridded data of vertical velocity at 300 hPa, geopotential height at 500 hPa, and u- and v-wind components at 850 hPa were obtained from the Climate Forecast System Reanalysis (CFSR; Saha et al. 2010), from which daily averages were calculated. Those variables were selected to connect the rainfall anomalies to large-scale circulations, and they were analyzed at 850, 500, and 300 hPa to represent the lower, middle, and upper troposphere. As with precipitation, composite standard anomalies were calculated for each of the above-mentioned atmospheric variables for the different MJO phases, and the statistical significance of those anomalies was computed using the Monte Carlo method described above. It should be noted that these composites were also performed using data from the European Centre for Medium-Range Weather Forecasts interim reanalysis (ERA-Interim; Dee et al. 2011), showing very similar patterns to those obtained with the CFSR.

The 1981–2010 period was used in the first part of the study to analyze the temporal and spatial variability of precipitation and the other atmospheric variables, because this is the period covered by the CFSR database. The 1981–2016 period, which corresponds to the CHIRPS database, was used in the second part of the analysis to investigate the influence of the MJO on the seasonal precipitation pattern in the MSD region in Mexico, when relative frequencies of the MJO phases were calculated for each date (MAX1, MIN, and MAX2).

3. Results

a. Spatiotemporal variability of summer precipitation in Mexico by MJO phase

Before considering MSD, it is important to first analyze the MJO's influence on precipitation over Mexico. Monthly composites of standardized precipitation anomalies binned according to MJO phase for all active MJO days (RMM ≥ 1) are shown in Figs. 2–4, and for inactive MJO days (RMM < 1) in Fig. 5.

1) WET PHASES

In general, positive standardized precipitation anomalies over Mexico and its Pacific and Gulf of Mexico coasts predominate when the enhanced MJO convective signal is found over the Western Hemisphere, Africa, or the Indian Ocean (i.e., phases 8, 1, and 2) during boreal summer (Fig. 2). Hereafter, these phases will be referred to as the wet phases.

Positive rainfall anomalies over the NETP, the Gulf of Mexico, and the Yucatan Peninsula are observed during phase 8 in June, August, September, and October. However, from July to September, negative rainfall anomalies are observed in areas of northern and central Mexico. During phase 1, positive rainfall anomalies are observed over southern Mexico, the NETP, and the Gulf of Mexico coasts. In September, these positive anomalies shift northward and cover the Baja California Peninsula. The strongest positive standardized anomalies during phase 1, in the range from +0.50 to +0.75, are
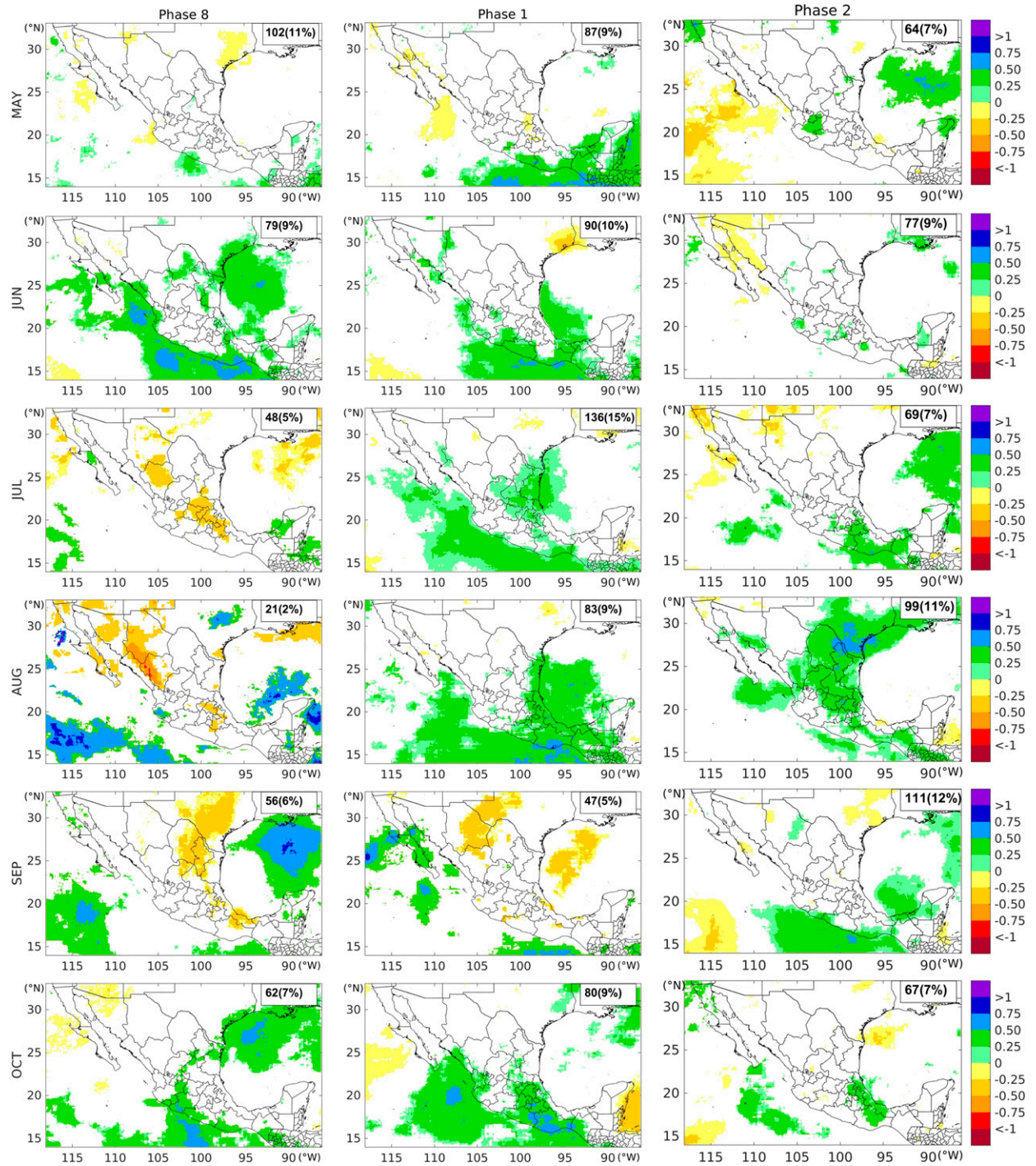
FIG. 2. Composites of standardized precipitation anomalies by MJO wet phases (8, 1, 2), for each month of the rainfall season (from May to October). The composites are based on 30 years (1981–2010) of daily data from the CHIRPS database. Only anomalies statistically significant at the 95% confidence level are displayed. The number of days considered for each composite and the percentages with respect to the total days of the period for each month are shown in the upper-right corners.

present over the southern states of Mexico in August and October. MJO phase 2 is also associated with enhanced precipitation over the study region; above-normal values predominate over the Mexican territory from July to October, but mainly in August when positive anomalies are observed in most of the country, reaching values from +0.50 to +0.75 in some regions of northeast Mexico.

2) DRY PHASES

In general, negative precipitation anomalies predominate over Mexico and its Pacific and Gulf of Mexico coasts when the enhanced MJO convective signal is located over the Maritime Continent or the western Pacific (i.e., phases 4–6) during boreal summer (Fig. 3). Hereafter, these phases will be referred to as the dry phases.

Negative rainfall anomalies are observed from May to October during MJO phase 4, mainly in the southern half of Mexico, the NETP, and the Gulf of Mexico (Fig. 3). During phase 5, negative anomalies are also observed over much of Mexico, with values from −0.25 to −0.50 covering large areas, particularly in July and August. However, positive anomalies from +0.25 to +0.50 are present over the northeast in June and October during phase 5. Below-normal rainfall anomalies persist into phase 6, although with lower magnitudes over Mexico when compared with phases 4 and 5. The pattern of negative anomalies is more consistent in the southern half of the country and the NETP, except during May.

3) TRANSITION PHASES

The summer rainfall anomalies in Mexico are more spatially variable when MJO is in phases 3 and 7, likely because these phases represent the transition between wet and dry conditions. Nevertheless, phase 3 is mainly associated with positive precipitation anomalies over the MSD region from July to September, while phase 7 is associated with negative anomalies mainly from June to August (Fig. 4).

The pattern of precipitation anomalies during phase 3 exhibits more variability from month to month during the rainy season compared to the rest of the MJO phases. The influence of phase 3 over the study region is more notable in June, July, September, and October; however, its impact on rainfall is spatially different throughout these months. For instance, strong positive anomalies from +0.50 to +0.75 or higher are notable in June, July, and September in some areas of the center, east, and northeast of Mexico, but inverse anomaly patterns are shown in July and September over some regions, like the Yucatan Peninsula, the Gulf of Mexico, and to the north of the country. Moreover, in contrast

with phases 8, 1, and 2, a large area with negative anomalies emerges in phase 3, covering northern regions in June and July, southeastern regions in September, and southwestern and central regions in October (Fig. 4).

As in phase 3, the influence of MJO phase 7 on the precipitation field in Mexico and adjacent coasts shows higher variability than other phases. For example, from June to August negative anomalies are observed in the southern half of Mexico, except the Yucatan Peninsula in August, but the anomaly pattern is not consistent in the rest of the months.

The composite maps of daily rainfall standardized anomalies from May to October for the inactive MJO category (amplitude less than 1) and the percentages of the number of days considered for each composite with respect to the total days of the period for each month are shown in Fig. 5. The inactive MJO signal is, in general, quite weak, although positive standardized anomalies predominate in May and negative in June over the MSD region of Mexico.

b. The MJO and the bimodal precipitation cycle in Mexico

The most frequent MJO phases during MAX1, MIN, and MAX2 in the region where the MSD occurs in Mexico are shown in Fig. 6. The results are only presented for those grid points in which the occurrence of the most frequent MJO phase was statistically significant, with respect to the other phases, at the 95% confidence level. The center panels in Fig. 6 show that during the relative minimum in rainfall the MJO phases that favor dry conditions in Mexico (phases 4–6) occur more frequently. This feature is more clearly observed over the southern half of Mexico (including the Yucatan Peninsula), but also in some areas to the northeast. It is a very consistent result that during the MIN the dry MJO phases occur more frequently, and even more taking into account that the amplitude of the MJO wave (both upward and downward branches) when over the equatorial Western Hemisphere is larger during June–August than during other months (Lafleur et al. 2015). Therefore, the MJO is likely contributing to the inhibition of precipitation in the middle of the rainy season by projecting this large-scale suppression onto other mechanisms reviewed in previous studies that generate and/or influence over the MSD. Thus, these MJO dry phases are strongly associated with the date of occurrence of the MSD minimum.

The MJO also influences the MAX2. Specifically, the MJO phases that favor wet conditions in Mexico (phases 8, 1, and 2), together with the transition phases, are the most frequent during the second peak of the rainfall
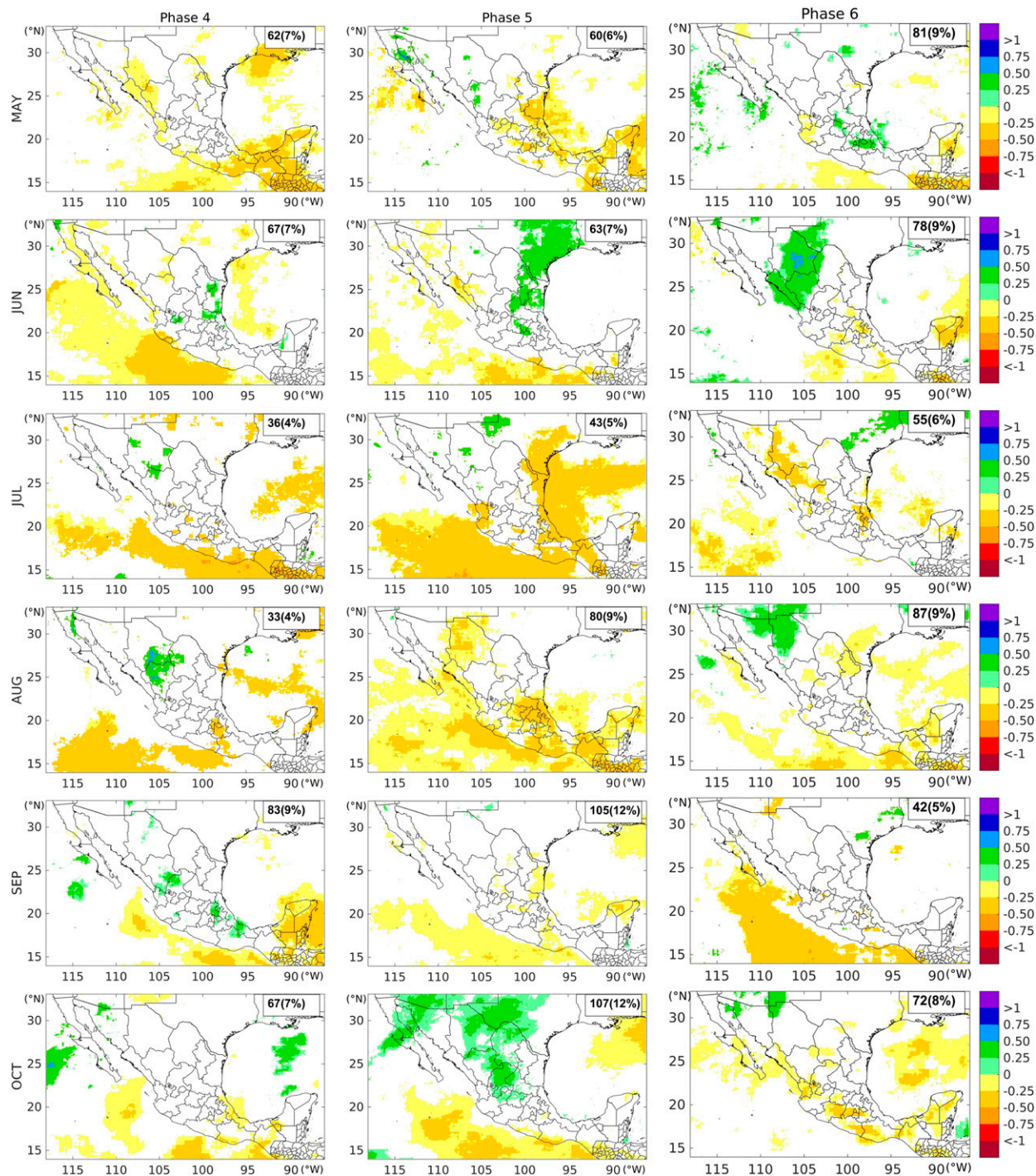
FIG. 3. As in Fig. 2, but for MJO dry phases (4–6).

season over the MSD region (Figs. 6c,f). MJO phase 3, which is the most frequent during MAX2, is associated with positive rainfall anomalies in September (one of the months when the second peak can occur except for the July-only MSD) and August (when the second peak in rainfall occurs during the July-only MSD) over the

MSD region, except in the Yucatan Peninsula in the latter (see Fig. 2). Phases 3 and 7 are the most frequent toward the east of the Yucatan Peninsula, in concordance with the positive precipitation anomalies observed in this region during October (the other month when MAX2 can occur for the August-only and the
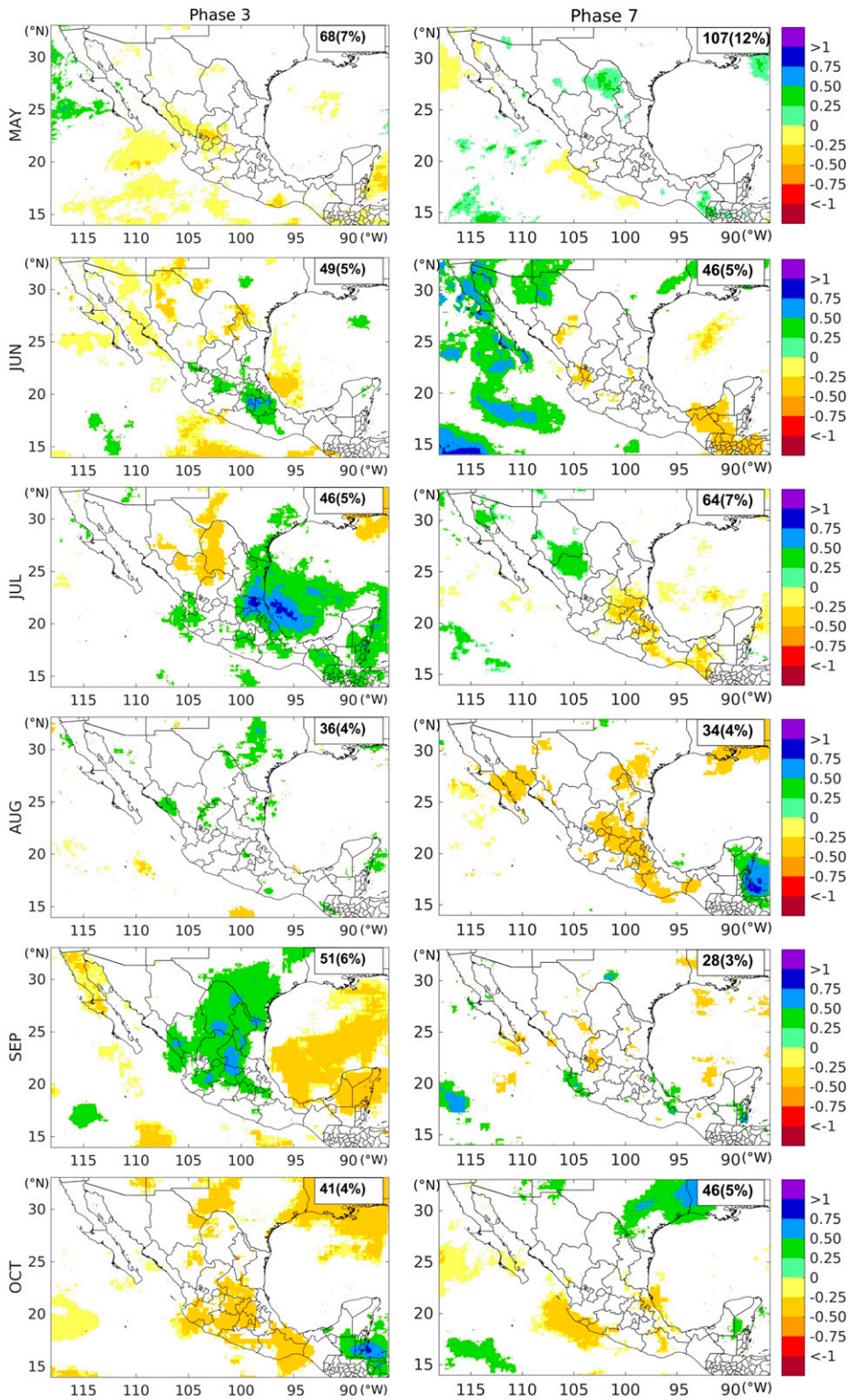
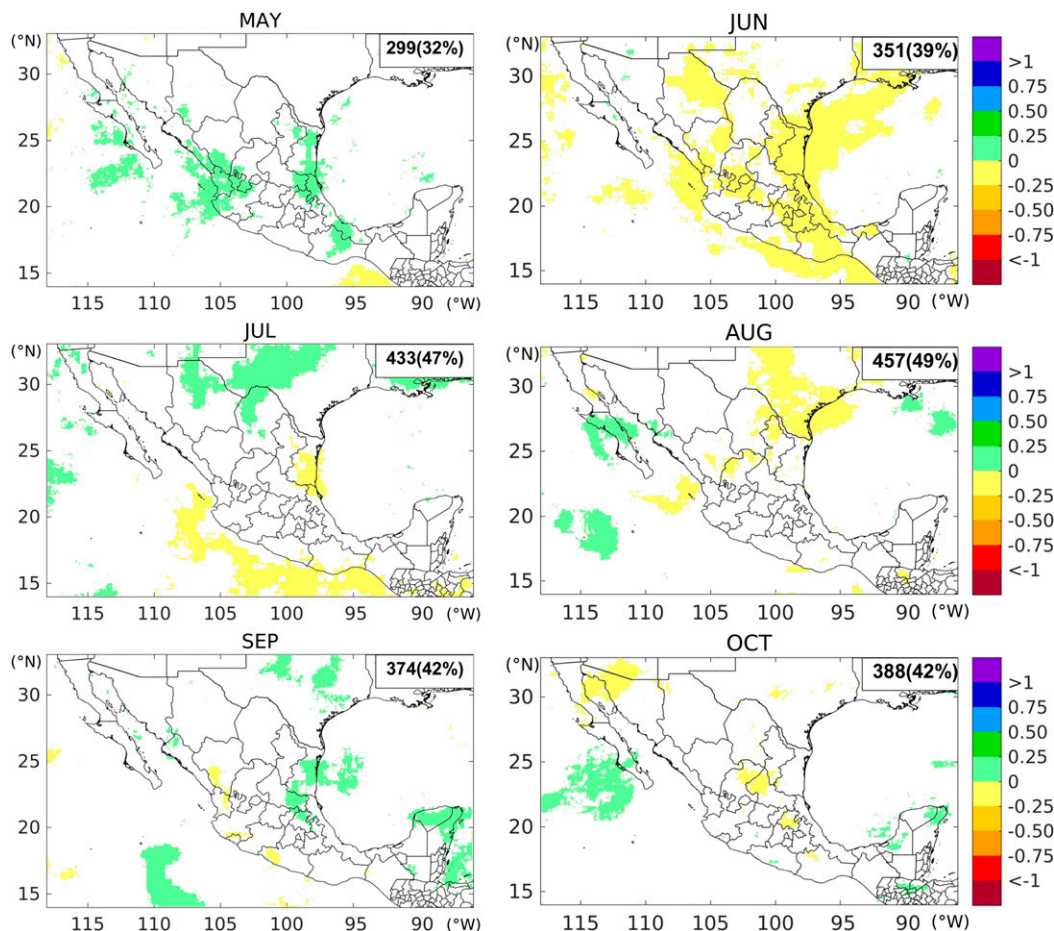FIG. 4. As in Fig. 2, but for MJO transition phases (3 and 7).

FIG. 5. As in Fig. 2, but for the inactive MJO category (RMM < 1).

July–August MSDs) (see Fig. 4). Therefore, via large-scale processes that favor precipitation (which are described in the next subsection), the MJO wet phases associate strongly with the date of occurrence of the MAX2.

On the other hand, the results suggest that the MJO is not strongly associated with an enhancement of convection and precipitation during MAX1 in Mexico (Figs. 6a,d). During this period, the pattern of the most frequent MJO phases shows more variability along the MSD region. The MJO wet phases are more frequent than the dry phases; however, the occurrence of dry phases (particularly phase 4) over the MSD region during MAX1 is not negligible. Furthermore, phase 7 also occurs with high frequency during MAX1, but this phase is associated with negative rainfall anomalies in June and July, when MAX1 occurs for the July-only, July–August, and August-only MSDs, respectively (see Fig. 4). The MJO contribution to the increase in rainfall amounts during the first rainfall peak is more evident over the southwest region of Mexico; in the rest of the MSD region the pattern is relatively noisy. Therefore,

the association of MJO with the first maximum of the rainfall season in Mexico appears to be mixed, perhaps leaning more toward a weakening of the bimodal pattern because of the inhibition of precipitation processes during MAX1 or toward a continuation of rainy conditions that prevent a clear transition from MAX1 to MIN.

ATMOSPHERIC CIRCULATION PATTERNS DURING SUMMER BY MJO PHASE

Anomaly composites of vertical velocity at 300 hPa, geopotential height at 500 hPa, and u- and v-wind components at 850 hPa for the MJO dry phases (4–6) during the MIN months (June–August), and for the wet phases (8, 1, and 2) during the MAX2 months (August–October), are presented in Figs. 7 and 8. The atmospheric circulation patterns are only presented for the MIN and MAX2 because no clear influence of the MJO on the date of MAX1 is observed. In general, the monthly anomaly patterns of these atmospheric variables for each MJO phase agree reasonably well with the rainfall anomaly patterns described in section 3a, in that
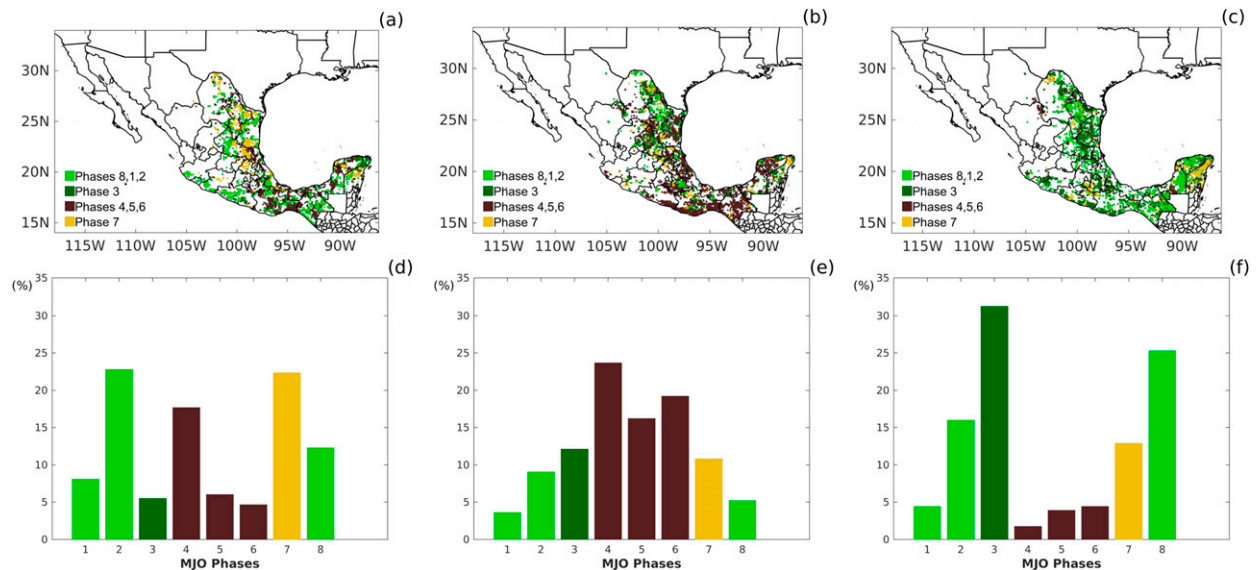
FIG. 6. (a)–(c) Spatial pattern and (d)–(f) frequency distributions of the more frequent MJO phases during (left) MAX1, (center) MIN, and (right) MAX2. The period considered was 1981–2016. Only frequencies statistically significant at the 95% confidence level are plotted.

atmospheric conditions during the wet phases generally favor convective precipitation processes while conditions during the dry phases do not (Figs. 7 and 8). When there are positive precipitation anomalies, negative geopotential height anomalies are observed in middle troposphere, and negative omega anomalies are present at 300 hPa, indicating upward vertical motion (Fig. 7). On the contrary, when negative rainfall anomalies are present, the atmospheric circulation patterns are generally inverse to those described above (Fig. 8).

During the MAX2, under the influence of wet phases, anomalous cyclonic circulations at 850 hPa centered over the NETP, and in some cases over the Gulf of Mexico (e.g., in August during phase 8, and in September during phases 8 and 2), are observed (Fig. 7). The associated 850-hPa wind anomalies from the southeast along the Pacific coast, from the southwest in the central and southern Mexico, and from the west in the NETP, favor moisture advection from the ocean into the continent (Fig. 7). Negative geopotential height anomalies at 500 hPa and upward vertical velocity anomalies are also observed in the region (Fig. 7). The inverse pattern is observed during the MIN, under the influence of dry phases (Fig. 8). The atmospheric circulation pattern in phase 8 for August differs from the rest of the wet phases in this month (Fig. 7), and is more related to that of MJO phase 7 (not shown).

The large cyclonic anomalies over the oceans during MAX2 in the wet phases (Fig. 7) tend to be associated with enhanced tropical cyclone activity in these basins (Barrett and Leslie 2009). It is recognized from previous studies that MJO modulates the intraseasonal variability

of convective activity over the tropical ocean (e.g., Maloney and Hartmann 2000a,b; Crosbie and Serra 2014). The MJO enhances cyclogenesis during the westerly phases of the MJO in the NETP and the Gulf of Mexico (Maloney and Hartmann 2000a,b), and hurricanes are over 4 times more numerous during these phases than during easterly phases in the NETP and tend to occur closer to the Mexican coast (Maloney and Hartmann 2000a). As stated in the introduction section, the summer rainfall regime in Mexico is influenced by the tropical cyclone activity. Because all of the above, tropical cyclones could be a reason for the stronger association of the MJO with the MAX2 compared to MAX1, when precipitation may still be connected to extratropical weather systems and when the frequency of tropical cyclones is lower.

As expected, for the inactive MJO category (Fig. 9), the 500-hPa geopotential height, 850-hPa wind vector, and 300-hPa pressure vertical velocity standardized anomalies are very weak. However, negative 500-hPa geopotential height anomalies are observed in May and positive ones are observed in June over Mexico, which are in agreement with the standardized precipitation anomalies obtained in these months in this MJO category (Fig. 5).

c. The MJO and the MSD duration in Mexico

The MJO associations presented above are more clearly observed in the July-only MSD (Fig. 10), where the dry phases are the most frequent during MIN (74% of the points) and the wet phases are the most frequent
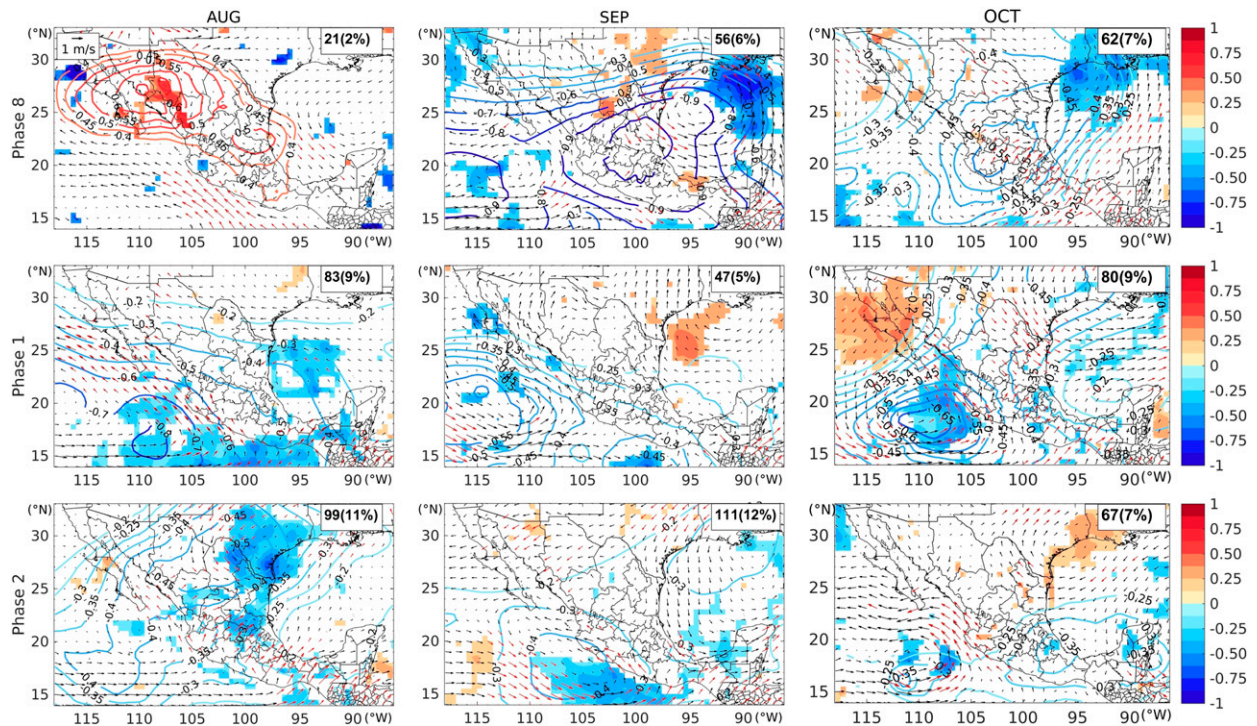
FIG. 7. Composites of standardized anomalies of 500-hPa geopotential height (color contours; negative anomalies in blue), 850-hPa wind vectors (red vectors indicate anomalies significant at the 95% confidence level), and 300-hPa pressure vertical velocity (shaded; negative anomalies in blue, indicating upward motion) for MJO wet phases (8, 1, 2) from August to October (MAX2 months). The composites are based on 30 years (1981–2010) of daily data from the CFSR. Only anomalies statistically significant at the 95% confidence level are plotted. The number of days considered in each composite and the percentages with respect to the total days of the period for each month are indicated in the upper-right corners.

during MAX2 (61% of the points). This pattern is also evident in the 2-month (July–August) MSD and in the August-only MSD, although the signal of these two types of MSD shows more regional variability when compared with the July-only MSD. Furthermore, very few statistically significant grid points are obtained in the 3-month MSD, found over extreme northeastern Mexico (see Fig. 1), and the occurrence of dry and wet phases is not consistent, except perhaps during MAX2 (Fig. 10). This lack of MJO–MSD association for the longer-duration MSD may be related to the MJO period: as a 30–60-day oscillation, the MJO may complete one or more full cycles during the longer MSD (2–3 months), thus complicating the relationship by promoting consecutive 5–10-day rainy periods, followed by 5–10-day dry periods.

Additionally, the MJO-related bimodal precipitation patterns identified previously are not always observed in regions of northeastern Mexico where MSD is present (e.g., in the July-only and the July–August MSDs during the MIN; or in the July–August MSD during the MAX2). These results suggest that the bimodal rainfall cycle is only slightly associated with the MJO in northeastern Mexico. It should be mentioned that this region

presents a very complex spatial structure and the highest interannual variability of the MSD (Perdigón-Morales et al. 2018), suggesting the influence of various processes, both local and large-scale forcing. In general, the relationship between the MJO and MSD is more consistent in the southern half of Mexico.

4. Discussion and conclusions

In this study, using a new precipitation database with very high spatial and temporal resolution, the influence of the MJO on summer rainfall in Mexico is examined. Particular emphasis is given to the MJO's association with the precipitation bimodal pattern whose spatial and temporal features were obtained from Perdigón-Morales et al. (2018), including the first (MAX1) and second (MAX2) maxima of the rainfall season and the minimum during the MSD (MIN).

The most important finding of this study is the impact of the MJO on the MIN and MAX2 during the rainy season. The dry (wet) MJO phases are the most frequent during the MIN (MAX2) over the MSD region in Mexico (Fig. 6). Thus, the MJO influences the intraseasonal pattern of precipitation by the inhibition
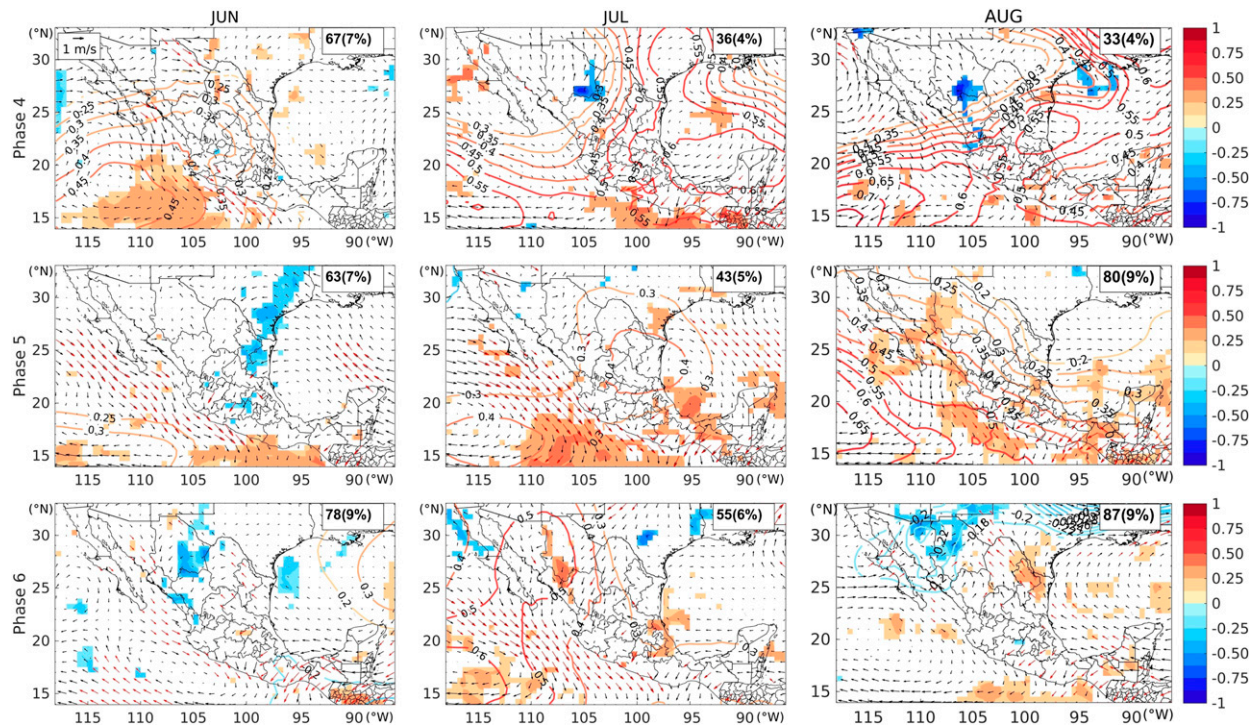
FIG. 8. As in Fig. 7, but for MJO dry phases (4–6) from June to August (MIN months).

(enhancement) of convection and precipitation during the MIN (MAX2). In contrast, the results suggest that MJO does not strongly favor convection and precipitation during the MAX1, but seems to suppress rainfall in most of the MSD region, except in southwestern Mexico in the August-only MSD (Fig. 10). Tropical cyclones could be a reason for the stronger association of the MJO with the date of MAX2 compared to MAX1 (in Fig. 7, see the cyclonic anomalies over the oceans from August to October). In addition, the MJO does not seem to influence the rainfall bimodal pattern over the northeastern region of Mexico, where the longest (June–August) MSD occurs. The MJO influence over the MIN and MAX2 is clearer in the southern half of Mexico, to the south of 22°N approximately (Fig. 6), and it is more evident in the 1- and 2-month MSDs (Fig. 10).

Anomalous anticyclonic circulations at 850 hPa and positive 500-hPa geopotential height anomalies are obtained over the region during the MSD under the influence of MJO dry phases (4–6) (Fig. 8). This atmospheric circulation pattern imposes northeasterly wind anomalies over southern Mexico and a low-level westward flow in the NETP, which restricts moisture advection toward the Mexican territory. On the contrary, anomalous cyclonic circulations at 850 hPa, negative 500-hPa geopotential height anomalies, 850-hPa northwesterly wind anomalies over the Yucatan Peninsula

and westerly and southwesterly wind anomalies over the central and southern Mexico, as well as low-level eastward flow in the NETP, all occur during MAX2 under the influence of MJO wet phases (8, 1, and 2) (Fig. 7). This atmospheric circulation pattern favors low-level moisture advection toward Mexico and, according to Maloney and Esbensen (2003), is in association with the MJO westerly wind anomalies in the lower atmosphere that transport heat and moisture from the east Pacific warm pool. This may intensify MJO convection, thereby creating a feedback loop that leads to further intensification of the local anomalous circulation and, therefore, of the convection processes observed in the region.

During different MJO phases, different atmospheric circulation patterns are present, either those that inhibit the precipitation processes over the MSD region of Mexico (such as during the MIN, when the MJO dry phases are more frequent) or those that favor them (such as during the MAX2, when the MJO wet phases are more frequent). However, the MJO in a given year could influence in the opposite sense: MJO wet phases (1 and 2) could weaken the processes that inhibit precipitation during the MIN (see in Fig. 7 the strong westerly anomalies in the NETP during these phases in August); while MJO dry phases (4–6) could weaken processes that favor precipitation during the MAX2 (see in Fig. 8 the strong easterly anomalies in the NETP
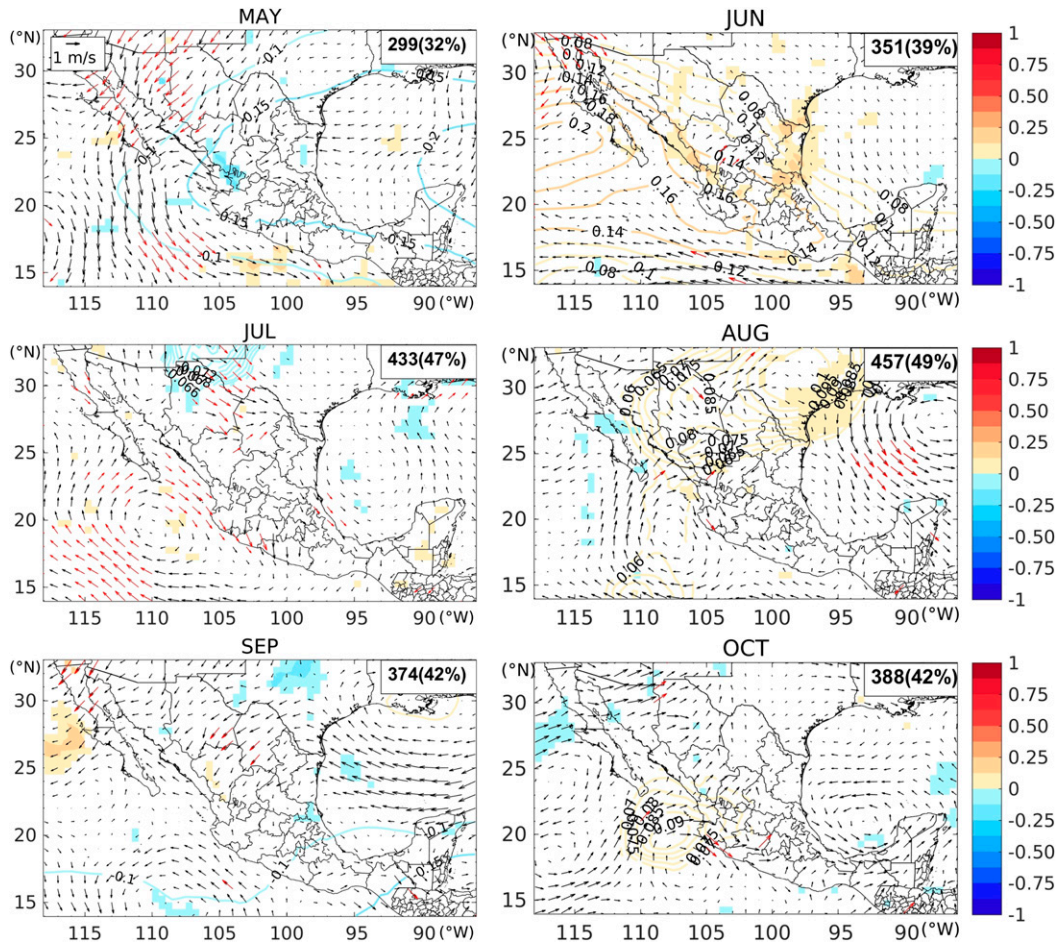
FIG. 9. As in Fig. 7, but for inactive MJO category (RMM < 1) from May to October.

during these phases in August). Thus, although the observed intraseasonal rainfall variation can be explained by changes in the convective and circulation patterns observed in association with the eastward propagation of the MJO, the pattern exhibits regional and temporal variability.

The mean atmospheric patterns that are present during the MSD period and during the second rainfall peak across the NETP and Mexico, which have been documented in previous studies (e.g., Romero-Centeno et al. 2007; Small et al. 2007), are modulated by the MJO. The mean circulation pattern obtained in the MSD period inhibits the northward extent of the southerly trades and restricts the low-level moisture transport into the continent. In addition, a westward low-level flow is observed in the NETP, which is associated with subsidence over southern Mexico and Central America. In MAX2, the northerly trades are weak, the southerly trades intensify and extend northeastward, and a low-level eastward flow in the NETP along with surface low pressure anomalies in the subtropical Atlantic and

Pacific are observed. The results presented here show that these mean atmospheric signals have been modulated by different phases of the MJO: the dry (wet) MJO phases strengthen (weakens) the former circulation pattern during the MIN, while the wet (dry) MJO phases strengthen (weaken) the latter during MAX2.

Despite the sometimes mixed signal, this analysis provides a valuable reference of the impact of each phase within a MJO cycle for each summer month (from May to October) over the study region. This study thus contributes to a better understanding of the rainfall intraseasonal variability in Mexico. Our results indicate a clear association between the MJO and summer precipitation in Mexico. Moreover, our results provide another important mechanism for the intraseasonal pattern of precipitation in the MSD region in Mexico that, heretofore, had not been considered for Mexico. This can be used to potentially improve extended forecasts, since the MJO may be predictable 2 or 3 weeks in advance once an event has started (e.g., Waliser et al. 2003).
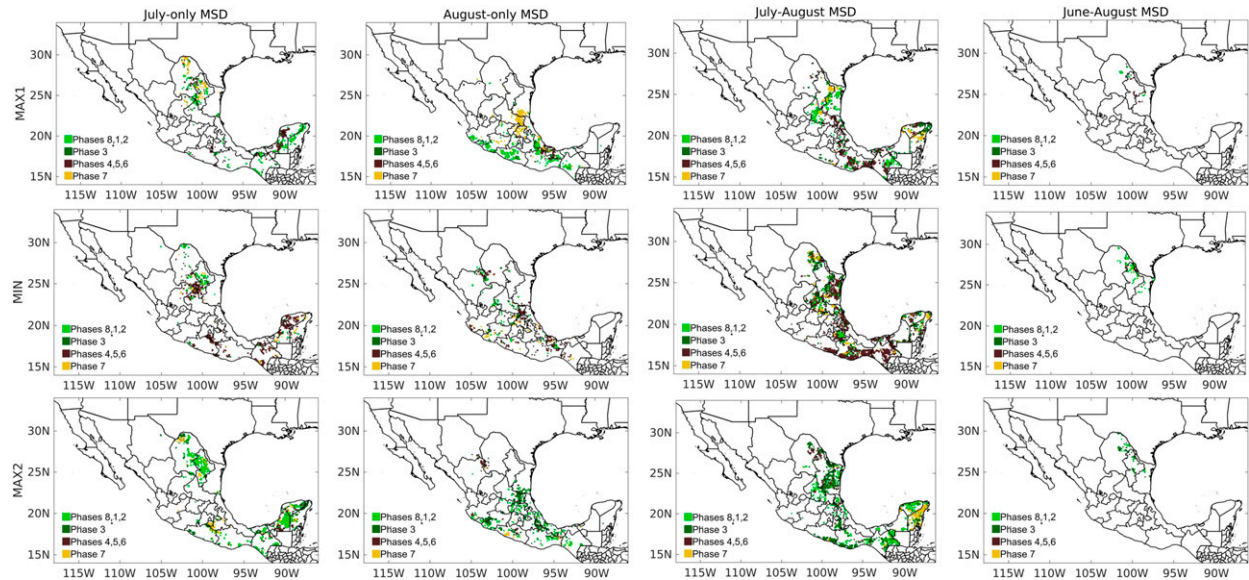
FIG. 10. Spatial pattern of the more frequent MJO phases during (top) MAX1, (middle) MIN, and (bottom) MAX2 for (left to right) July-only MSD, August-only MSD, July–August MSD, and the June–August MSD. The period considered was 1981–2016. Only frequencies statistically significant at the 95% confidence level are plotted.

REFERENCES

Alvarez, M. S., C. S. Vera, G. N. Kiladis, and B. Liebmann, 2016: Influence of the Madden–Julian Oscillation on precipitation and surface air temperature in South America. *Climate Dyn.*, **46**, 245–262, https://doi.org/10.1007/s00382-015-2581-6.

Amador, J. A., E. J. Alfaro, O. G. Lizano, and V. O. Magaña, 2006: Atmospheric forcing of the eastern tropical Pacific: A review. *Prog. Oceanogr.*, **69**, 101–142, https://doi.org/10.1016/j.pocean.2006.03.007.

Barlow, M., and D. Salstein, 2006: Summertime influence of the Madden–Julian oscillation on daily rainfall over Mexico and Central America. *Geophys. Res. Lett.*, **33**, L21708, https://doi.org/10.1029/2006GL027738.

Barrett, B. S., and L. M. Leslie, 2009: Links between tropical cyclone activity and Madden–Julian oscillation phase in the North Atlantic and northeast Pacific basins. *Mon. Wea. Rev.*, **137**, 727–744, https://doi.org/10.1175/2008MWR2602.1.

——, and M. I. Esquivel, 2013: Variability of precipitation and temperature in Guanajuato, Mexico. *Atmósfera*, **26**, 521–536, https://doi.org/10.1016/S0187-6236(13)71093-2.

——, and G. B. Raga, 2016: Variability of winter and summer surface ozone in Mexico City on the intraseasonal timescale. *Atmos. Chem. Phys.*, **16**, 15 359–15 370, https://doi.org/10.5194/acp-16-15359-2016.

——, J. F. Carrasco, and A. P. Testino, 2012: Madden–Julian oscillation (MJO) modulation of atmospheric circulation and Chilean winter precipitation. *J. Climate*, **25**, 1678–1688, https://doi.org/10.1175/JCLI-D-11-00216.1.

Bond, N. A., and G. A. Vecchi, 2003: The influence of the Madden–Julian oscillation on precipitation in Oregon and Washington. *Wea. Forecasting*, **18**, 600–613, https://doi.org/10.1175/1520-0434(2003)018<0600:TIOTMO>2.0.CO;2.

Crosbie, E., and Y. Serra, 2014: Intraseasonal modulation of synoptic-scale disturbances and tropical cyclone genesis in the eastern North Pacific. *J. Climate*, **27**, 5724–5745, https://doi.org/10.1175/JCLI-D-13-00399.1.

Curtis, S., 2002: Interannual variability of the bimodal distribution of summertime rainfall over Central America and tropical storm activity in the far-eastern Pacific. *Climate Res.*, **22**, 141–146, https://doi.org/10.3354/cr022141.

——, and D. W. Gamble, 2008: Regional variations of the Caribbean mid-summer drought. *Theor. Appl. Climatol.*, **94**, 25–34, https://doi.org/10.1007/s00704-007-0342-0.

——, and ——, 2016: The boreal winter Madden–Julian Oscillation's influence on summertime precipitation in the greater Caribbean. *J. Geophys. Res. Atmos.*, **121**, 7592–7605, https://doi.org/10.1002/2016JD025031.

Dee, D. P., and Coauthors, 2011: The ERA-Interim reanalysis: Configuration and performance of the data assimilation system. *Quart. J. Roy. Meteor. Soc.*, **137**, 553–597, https://doi.org/10.1002/qj.828.

Efron, B., and R. J. Tibshirani, 1994: *An Introduction to the Bootstrap*. CRC Press, 430 pp.

Funk, C. C., and Coauthors, 2015: The climate hazards infrared precipitation with stations—A new enviromental record for monitoring extremes. *Sci. Data*, **2**, 150066, https://doi.org/10.1038/sdata.2015.66 (2015).

Gamble, D. W., D. B. Parnell, and S. Curtis, 2008: Spatial variability of the Caribbean mid-summer drought and relation to North Atlantic high circulation. *Int. J. Climatol.*, **28**, 343–350, https://doi.org/10.1002/joc.1600.

Giannini, A., Y. Kushnir, and M. A. Cane, 2000: Interannual variability of Caribbean rainfall, ENSO, and the Atlantic Ocean. *J. Climate*, **13**, 297–311, https://doi.org/10.1175/1520-0442(2000)013<0297:IVOCRE>2.0.CO;2.

Hall, J. D., A. J. Matthews, and D. J. Karoly, 2001: The modulation of tropical cyclone activity in the Australian region by the Madden–Julian oscillation. *Mon. Wea. Rev.*, **129**, 2970–2982, https://doi.org/10.1175/1520-0493(2001)129<2970:TMOTCA>2.0.CO;2.

Hendon, H. H., and M. L. Salby, 1994: The life cycle of the Madden–Julian oscillation. *J. Atmos. Sci.*, **51**, 2225–2237, https://doi.org/10.1175/1520-0469(1994)051<2225:TLCOTM>2.0.CO;2.

Herrera, E., V. Magaña, and E. Caetano, 2015: Air–sea interactions and dynamical processes associated with the midsummer drought. *Int. J. Climatol.*, **35**, 1569–1578, https://doi.org/10.1002/joc.4077.

Higgins, R., and W. Shi, 2001: Intercomparison of the principal modes of interannual and intraseasonal variability of the North American monsoon system. *J. Climate*, **14**, 403–417, https://doi.org/10.1175/1520-0442(2001)014<0403:IOTPMO>2.0.CO;2.

Karnauskas, K. B., R. Seager, A. Giannini, and A. J. Busalacchi, 2013: A simple mechanism for the climatological midsummer drought along the Pacific coast of Central America. *Atmósfera*, **26**, 261–281, https://doi.org/10.1016/S0187-6236(13)71075-0.

Katsanos, D., A. Retalis, and S. Michaelides, 2016: Validation of a high-resolution precipitation database (CHIRPS) over Cyprus for a 30-year period. *Atmos. Res.*, **169**, 459–464, https://doi.org/10.1016/j.atmosres.2015.05.015.

Klotzbach, P. J., 2010: On the Madden–Julian oscillation–Atlantic hurricane relationship. *J. Climate*, **23**, 282–293, https://doi.org/10.1175/2009JCLI2978.1.

Lafleur, D. M., B. S. Barrett, and G. R. Henderson, 2015: Some climatological aspects of the Madden–Julian oscillation (MJO). *J. Climate*, **28**, 6039–6053, https://doi.org/10.1175/JCLI-D-14-00744.1.

López-Carr, D., and Coauthors, 2015: A spatial analysis of climate-related child malnutrition in the Lake Victoria Basin. *2015 IEEE Int. Geoscience and Remote Sensing Symposium (IGARSS)*, Milan, Italy, IEEE, 2564–2567, https://doi.org/10.1109/IGARSS.2015.7326335.

Madden, R. A., and P. R. Julian, 1994: Observations of the 40–50 day tropical oscillation—A review. *Mon. Wea. Rev.*, **122**, 814–837, https://doi.org/10.1175/1520-0493(1994)122<0814:OOTDTO>2.0.CO;2.

Magaña, V., and E. Caetano, 2005: Temporal evolution of summer convective activity over the Americas warm pools. *Geophys. Res. Lett.*, **32**, L02803, https://doi.org/10.1029/2004GL021033.

——, J. A. Amador, and S. Medina, 1999: The midsummer drought over Mexico and Central America. *J. Climate*, **12**, 1577–1588, https://doi.org/10.1175/1520-0442(1999)012<1577:TMDOMA>2.0.CO;2.

Maldonado, T., A. Rutgersson, E. Alfaro, J. Amador, and B. Claremar, 2016: Interannual variability of the midsummer drought in Central America and the connection with sea surface temperatures. *Adv. Geosci.*, **42**, 35–50, https://doi.org/10.5194/adgeo-42-35-2016.

Maloney, E. D., and D. L. Hartmann, 2000a: Modulation of eastern North Pacific hurricanes by the Madden–Julian oscillation. *J. Climate*, **13**, 1451–1460, https://doi.org/10.1175/1520-0442(2000)013<1451:MOENPH>2.0.CO;2.

——, and ——, 2000b: Modulation of hurricane activity in the Gulf of Mexico by the Madden–Julian oscillation. *Science*, **287**, 2002–2004, https://doi.org/10.1126/science.287.5460.2002.

——, and S. K. Esbensen, 2003: The amplification of east Pacific Madden–Julian oscillation convection and wind anomalies during June–November. *J. Climate*, **16**, 3482–3497, https://doi.org/10.1175/1520-0442(2003)016<3482:TAOEPM>2.0.CO;2.

Mapes, B. E., P. Liu, and N. Buenning, 2005: Indian monsoon onset and the Americas midsummer drought: Out-of-equilibrium responses to smooth seasonal forcing. *J. Climate*, **18**, 1109–1115, https://doi.org/10.1175/JCLI-3310.1.

Martin, E. R., and C. Schumacher, 2011: Modulation of Caribbean precipitation by the Madden–Julian oscillation. *J. Climate*, **24**, 813–824, https://doi.org/10.1175/2010JCLI3773.1.

Mo, K. C., 2000: Intraseasonal modulation of summer precipitation over North America. *Mon. Wea. Rev.*, **128**, 1490–1505, https://doi.org/10.1175/1520-0493(2000)128<1490:IMOSPO>2.0.CO;2.

Ordoñez, P., P. Ribera, D. Gallego, and C. Peña-Ortiz, 2013: Influence of Madden–Julian Oscillation on water budget transported by the Somali low-level jet and the associated Indian summer monsoon rainfall. *Water Resour. Res.*, **49**, 6474–6485, https://doi.org/10.1002/wrcr.20515.

Paredes-Trejo, F. J., H. Álvarez-Barbosa, M. A. Peñaloza-Murillo, M. A. Moreno, and A. Farias, 2016: Intercomparison of improved satellite rainfall estimation with CHIRPS gridded product and rain gauge data over Venezuela. *Atmósfera*, **29**, 323–342, https://doi.org/10.20937/ATM.2016.29.04.04.

Perdigón-Morales, J., R. Romero-Centeno, P. Ordóñez Pérez, and B. S. Barrett, 2018: The midsummer drought in Mexico: Perspectives on duration and intensity from the CHIRPS precipitation database. *Int. J. Climatol.*, **38**, 2174–2186, https://doi.org/10.1002/joc.5322.

Romero-Centeno, R., J. Zavala-Hidalgo, and G. B. Raga, 2007: Midsummer gap winds and low-level circulation over the eastern tropical Pacific. *J. Climate*, **20**, 3768–3784, https://doi.org/10.1175/JCLI4220.1.

Saha, S., and Coauthors, 2010: NCEP Climate Forecast System Reanalysis (CFSR) Selected Hourly Time-Series Products, January 1979 to December 2010. NCAR Computational and Information Systems Laboratory Research Data Archive, accessed 14 March 2018, https://doi.org/10.5065/D6513W89.

Shimizu, M. H., T. Ambrizzi, and B. Liebmann, 2017: Extreme precipitation events and their relationship with ENSO and MJO phases over northern South America. *Int. J. Climatol.*, **37**, 2977–2989, https://doi.org/10.1002/joc.4893.

Small, R. J., S. P. Szoeke, and S. P. Xie, 2007: The Central American midsummer drought: Regional aspects and large-scale forcing. *J. Climate*, **20**, 4853–4873, https://doi.org/10.1175/JCLI4261.1.

Verdin, A., C. Funk, B. Rajagopalan, and W. Kleiber, 2016: Kriging and local polynomial methods for blending satellite-derived and gauge precipitation estimates to support hydrologic early warning systems. *IEEE Trans. Geosci. Remote Sens.*, **54**, 2552–2562, https://doi.org/10.1109/TGRS.2015.2502956.

Waliser, D. E., K. M. Lau, W. Stern, and C. Jones, 2003: Potential predictability of the Madden–Julian Oscillation. *Bull. Amer. Meteor. Soc.*, **84**, 33–50, https://doi.org/10.1175/BAMS-84-1-33.

Wheeler, M. C., and H. H. Hendon, 2004: An all-season real-time multivariate MJO index: Development of an index for monitoring and prediction. *Mon. Wea. Rev.*, **132**, 1917–1932, https://doi.org/10.1175/1520-0493(2004)132<1917:AARMMI>2.0.CO;2.

Whitaker, J. W., and E. D. Maloney, 2018: Influence of the Madden–Julian Oscillation and Caribbean low-level jet on east Pacific easterly wave dynamics. *J. Atmos. Sci.*, **75**, 1121–1141, https://doi.org/10.1175/JAS-D-17-0250.1.

Zhang, C., 2005: Madden–Julian oscillation. *Rev. Geophys.*, **43**, RG2003, https://doi.org/10.1029/2004RG000158.

Zhou, S., M. L'Heureux, S. Weaver, and A. Kumar, 2012: A composite study of the MJO influence on the surface air temperature and precipitation over the continental United States. *Climate Dyn.*, **38**, 1459–1471, https://doi.org/10.1007/s00382-011-1001-9.